J. Phys. Chem. A **1998,** *102,* 7964−7974

Atmospheric Chemistry of the Phenoxy Radical, $C_6H_5O(\bullet)$: UV Spectrum and Kinetics of Its Reaction with NO, NO_2, and O_2

J. Platz and O. J. Nielsen[†]

Atmospheric Chemistry, Plant Biology and Biogeochemistry Department, Risø National Laboratory,
DK-4000, Roskilde, Denmark

T. J. Wallington,*,[‡] **J. C. Ball, M. D. Hurley, A. M. Straccia, and W. F. Schneider**

Ford Motor Company, 20000 Rotunda Drive, Mail Drop SRL-3083, Dearborn, Michigan 48121-2053

J. Sehested[§]

Haldor Topsoe A/S, Nymoellevej 55, DK-2800 Lyngby, Denmark

Received: May 12, 1998; In Final Form: June 29, 1998

Pulse radiolysis and FT-IR smog chamber experiments were used to investigate the atmospheric fate of $C_6H_5O(\bullet)$ radicals. Pulse radiolysis experiments gave $\sigma(C_6H_5O(\bullet))_{235\ \mathrm{nm}} = (3.82 \pm 0.48) \times 10^{-17}$ cm^2 molecule^{-1}, $k(C_6H_5O(\bullet) + NO) = (1.88 \pm 0.16) \times 10^{-12}$, and $k(C_6H_5O(\bullet) + NO_2) = (2.08 \pm 0.15) \times 10^{-12}$ cm^3 molecule^{-1} s^{-1} at 296 K in 1000 mbar of SF_6 diluent. No discernible reaction of $C_6H_5O(\bullet)$ radicals with O_2 was observed in smog chamber experiments, and we derive an upper limit of $k(C_6H_5O(\bullet) + O_2) < 5 \times 10^{-21}$ cm^3 molecule^{-1} s^{-1} at 296 K. These results imply that the atmospheric fate of phenoxy radicals in urban air masses is reaction with NO_x. Density functional calculations and gas chromatography−mass spectrometry are used to identify 4-phenoxyphenol as the major product of the self-reaction of $C_6H_5O(\bullet)$ radicals. As part of this study, relative rate techniques were used to measure rate constants for reaction of Cl atoms with phenol [$k(Cl + C_6H_5OH) = (1.93 \pm 0.36) \times 10^{-10}$], several chlorophenols [k(Cl + 2-chlorophenol) = $(7.32 \pm 1.30) \times 10^{-12}$, k(Cl + 3-chlorophenol) = $(1.56 \pm 0.21) \times 10^{-10}$, and k(Cl + 4-chlorophenol) = $(2.37 \pm 0.30) \times 10^{-10}$], and benzoquinone [$k$(Cl + benzoquinone) = $(1.94 \pm 0.35) \times 10^{-10}$], all in units of cm^3 molecule^{-1} s^{-1}. A reaction between molecular chlorine and C_6H_5OH to produce 2- and 4-chlorophenol in yields of (28 ± 3)% and (75 ± 4)% was observed. This reaction is probably heterogeneous in nature, and an upper limit of $k(Cl_2 + C_6H_5OH) \leq 1.9 \times 10^{-20}$ cm^3 molecule^{-1} s^{-1} was established for the homogeneous component. These results are discussed with respect to the previous literature data and to the atmospheric chemistry of aromatic compounds.

1. Introduction

Aromatic compounds such as toluene, ethyl benzene, and the xylenes are important constituents of automotive gasoline. Typical gasoline blends currently sold in the United States have an aromatic content of 20−30% by volume.[1] It is well-established that aromatic species are important components of automobile tailpipe exhaust and evaporative emissions and contribute to formation of ozone[2] and secondary organic aerosol[3] in urban air. Unfortunately, our understanding of the atmospheric chemistry of aromatic compounds is incomplete, and assessments of the environmental impact of the atmospheric release of such species are uncertain.

One experimental problem associated with the study of the atmospheric chemistry of aromatic compounds is the scarcity of sources for the intermediate radical species that are formed in the sequence of oxidation reactions. Fortunately, this limitation has been lifted partially by recent reports of a convenient source for the phenoxy radical, $C_6H_5O(\bullet)$, namely, reaction of Cl atoms with C_6H_5OH.[4−6]

Berho and Lesclaux[5] used reaction 1 as a source of phenoxy radicals in their flash photolysis study of the kinetics of reactions 2 and 3.

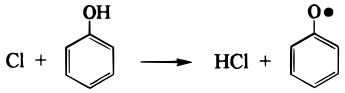

(1)

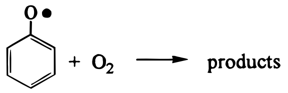

(2)

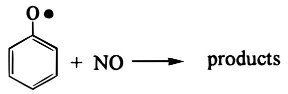

(3)

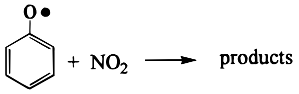

(4)

No reaction between phenoxy radicals and O_2 was observed by Berho and Lesclaux,[5] and an upper limit of $k_2 < 2 \times 10^{-18}$

[†] E-mail: ole.john.nielsen@risoe.dk.

[‡] E-mail: twalling@ford.com.

[§] E-mail: jss@topsoe.dk.

S1089-5639(98)02221-X CCC: $15.00

cm^3 molecule^{-1} s^{-1} for temperatures up to 500 K was reported. This upper limit, while clearly indicating a very slow reaction, does not preclude the possibility that reaction 2 is an important atmospheric fate for phenoxy radicals. Berho and Lesclaux[5] reported that reaction 3 proceeds at a moderate rate with $k_3 = 1.7 \times 10^{-12}$ cm^3 molecule^{-1} s^{-1} at 293 K. To provide further information concerning the atmospheric fate of $C_6H_5O(\bullet)$ radicals, we have conducted experiments using pulse radiolysis and smog chamber facilities to study the kinetics of reaction 2, 3, and 4.

During the course of the experimental work, it became necessary to study the kinetics and mechanism of the reactions of molecular and atomic chlorine with C_6H_5OH, the three chlorophenol isomers, and benzoquinone (a possible oxidation product of phenol). The results of these additional studies are reported here. We also consider the fate of $C_6H_5O(\bullet)$ radicals produced in the smog chamber experiments. Density functional calculations were used to investigate the thermodynamics and vibrational spectra of possible reactions products, including the hypochlorite C_6H_4OCl, the peroxide $C_6H_5OOC_6H_5$, the ether 4-$C_6H_5OC_6H_4OH$, and the biphenyl 4,4′-$HOC_6H_4C_6H_4OH$. Formation of the former two is predicted to be thermodynamically unfavorable, while the latter two are probable products of $C_6H_5O(\bullet)$ radical self-reaction. Coupled gas chromatography−mass spectrometry experiments confirm that 4-phenoxyphenol is the main product of self-reaction, with at least three other minor products also present.

2. Experimental Section

Two experimental systems were used; both are described elsewhere.[7,8] All experiments were performed at 296 K. All uncertainties reported in this paper are 2 standard deviations. Standard error propagation methods were used where appropriate.

2.1. Pulse Radiolysis System. Phenoxy radicals were generated by the radiolysis of $SF_6/HCl/C_6H_5OH$ gas mixtures in a 1 L stainless steel reaction cell with a 30 ns pulse of 2 MeV electrons from a Febetron 705 field emission accelerator. SF_6 was always in great excess and was used to generate fluorine atoms:

$$SF_6 \xrightarrow{2\ \mathrm{MeV}\ e^-} F + \text{products} \tag{5}$$

$$F + HCl \longrightarrow HF + Cl \tag{6}$$

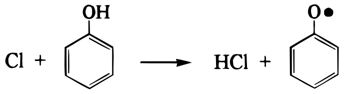

(7)

The radiolysis dose was varied by insertion of stainless steel attenuators between the accelerator and the reaction cell. In this work we refer to the radiolysis dose as a fraction of the maximum dose that is achievable. The fluorine atom yield was calibrated by monitoring the transient absorption at 260 nm by CH_3O_2 radicals produced by pulse radiolysis of $SF_6/CH_4/O_2$ mixtures. Using $\sigma(CH_3O_2) = 3.18 \times 10^{-18}$ cm^2 molecule^{-1},[9] the F atom yield was determined to be $(2.98 \pm 0.34) \times 10^{15}$ molecule cm^{-3} at full radiolysis dose and 1000 mbar of SF_6. The quoted error includes 10% uncertainty in $\sigma(CH_3O_2)$.

The analysis light was provided by a 150 W pulsed xenon arc lamp and was multipassed through the reaction cell using internal White cell optics to give total optical path length of 80 cm. After leaving the cell, the light was guided through a monochromator and detected with either a photomultiplier to record absorption transients or a diode array camera to record UV absorption spectra. All absorption transients were derived from single-pulse experiments. The spectral resolution was 0.8 nm with the photomultiplier detector and 3.2 nm with the diode array.

Reagent concentrations used were: SF_6, 980−1000 mbar; HCl, 20 mbar; C_6H_5OH, 0.1 mbar; NO, 1−5 mbar; NO_2, 1−4 mbar. All experiments were performed at 296 K and 1000 mbar total pressure. Chemicals were supplied by SF_6 (99.9%) Gerling and Holz; C_6H_5OH (>99.8%) Merck; NO_2 (>98%) Linde Technische Gase; NO (99.8%) Messer Griesheim. The C_6H_5OH sample was subject to freeze−pump−thaw cycling before use. All other chemicals were used as received.

Two sets of experiments were performed using the pulse radiolysis system. First, the UV absorption spectrum of the phenoxy radical was recorded using the diode array camera to capture the UV absorption following radiolysis of $SF_6/HCl/C_6H_5OH$ mixtures. Second, the rate constants for reactions 3 and 4 were determined from the decay of the absorption at 235 nm (attributed to the $C_6H_5O(\bullet)$ radical) following radiolysis of $SF_6/HCl/C_6H_5OH/NO$ and $SF_6/HCl/C_6H_5OH/NO_2$ mixtures.

2.2. FT-IR Smog Chamber System. FT-IR smog chamber techniques were used to study the reactions of (i) molecular chlorine with C_6H_5OH, (ii) atomic chlorine with C_6H_5OH, benzoquinone, and the three chlorophenol isomers, and (iii) phenoxy radicals with O_2. Experiments were conducted using a 140 L Pyrex reaction chamber[8] interfaced to an FT-IR spectrometer for in situ chemical analysis. GC−MS was also used for product analysis. Prior to GC−MS analysis, the chamber contents were pumped slowly through a cold trap maintained at 0 °C. The condensate was dissolved in methylene chloride and analyzed with a Finnigan MAT GCQ GC/MS system using a Restec Rtx-5ms 30 m capillary column. Individual compounds were resolved using a program that increased the temperature of the column from 40 to 300 °C at a rate of 10 °C/min.

Radicals were generated by UV irradiation (22 black lamps) of mixtures of 3−10 mTorr of reactant (C_6H_5OH, benzoquinone, 2-, 3- or 4-chlorophenol) and 0.003−1.2 Torr of Cl_2 in 700 Torr of N_2, air, or O_2 diluents at 296 K (760 Torr = 1013 mbar = 101 kPa). Reactant loss and product formation were monitored by FT-IR spectroscopy using their characteristic features over the wavenumber range 800−2000 cm^{-1}. The analyzing path length for the FT-IR system was 28 m, and the spectral resolution was 0.25 cm^{-1}. Infrared spectra were derived from 32 coadded spectra.

2.3. Density Functional Calculations. Electronic structure calculations were performed using the Amsterdam Density Functional (ADF) code.[10] Geometries and vibrational spectra were first determined within the local (spin) density approximation (L(S)DA),[11] the latter by two-sided differentiation of the analytical energy gradients. Final geometries and energies were obtained within the generalized gradient approximation of Perdew and Wang (PW91).[12] A valence double-ζ plus polarization Slater-type basis was used for all atoms. The numerical integration mesh parameter, which determines the approximate number of significant digits in the internal numerical integrations in ADF, was set to 6.0.[10b] With these mesh parameters, total energies are converged to <0.1 kcal mol^{-1} and geometries to <0.001 Å. Geometries were converged to maximum and root-mean-square gradients of less than 10^{-4} and 4×10^{-5} hartree a_0^{-1}, respectively. Zero-point energies were calculated from the unscaled LSDA frequencies. Enthalpy corrections to 298

K were calculated using standard formulas, with vibrations <260 cm^{-1} treated as free rotations.

3. Results and Discussion

3.1. UV Spectrum of the $C_6H_5O(\bullet)$ Radical. The pulsed radiolysis of mixtures of 980 mbar SF_6, 20 mbar HCl, and 0.1 mbar C_6H_5OH was used to record the UV spectrum of the $C_6H_5O(\bullet)$ radical. Immediately after the radiolysis pulse, a rapid (complete within 2−3 μs) increase in absorption was observed at 235 nm, followed by a slower decay. We ascribe the absorption to the formation of $C_6H_5O(\bullet)$ radicals. No absorption was observed when either 1000 mbar of SF_6, 20 mbar of HCl, or 0.1 mbar of C_6H_5OH was radiolyzed separately. HCl and C_6H_5OH compete for the F atoms produced by radiolysis of SF_6. F atoms react with HCl with a rate constant of $k_6 = 1.2 \times 10^{-11}$ cm^3 $molecule^{-1}$ s^{-1}.[13] There are no literature data concerning the kinetics of the reaction of F atoms with phenol. To obtain a rate constant for the reaction of F atoms with C_6H_5OH, mixtures of SF_6 and C_6H_5OH were subjected to pulse radiolysis and the rate of formation of $C_6H_5O(\bullet)$ radicals was measured as a function of the C_6H_5OH concentration. From the rate of appearance of the phenoxy radicals, a value of $k(F + C_6H_5OH) = (3.1 \pm 0.3) \times 10^{-10}$ cm^3 $molecule^{-1}$ s^{-1} was established.

In our experiments using $SF_6/C_6H_5OH/HCl$ mixtures, the concentration of HCl was 200 times that of C_6H_5OH and approximately 89% of the F atoms will be converted into Cl atoms via reaction 6 while 11% will react directly with C_6H_5OH. Reaction of Cl atoms with C_6H_5OH is a clean source of phenoxy radicals.[4−6] In contrast, F atoms generally react with aromatic compounds via two pathways: H atom abstraction and adduct formation. To assess the potential complications caused by reaction of F atoms with C_6H_5OH, additional experiments were performed using mixtures of 1000 mbar of SF_6 and 0.1 mbar of C_6H_5OH. The UV absorption spectra obtained from experiments employing SF_6/C_6H_5OH and $SF_6/HCl/C_6H_5OH$ mixtures were similar in all respects except one: the presence of a broad feature at 300−340 nm in the spectra obtained using SF_6/C_6H_5OH mixtures, which we attribute to the $F-C_6H_5OH$ adduct. Comparing the yields at 235 nm using F and Cl atoms for phenoxy radical formation, we conclude that a substantial fraction (≈45%) of the reaction of F atoms with C_6H_5OH produces $C_6H_5O(\bullet)$ radicals and that the UV absorption spectra obtained using $SF_6/HCl/C_6H_5OH$ mixtures are free from significant complications associated with the formation of the $F-C_6H_5OH$ adduct.

To provide an absolute calibration for the $C_6H_5O(\bullet)$ radical spectrum, it is important to work under conditions where 100% of the Cl atoms are converted into $C_6H_5O(\bullet)$ radicals. It is necessary to consider potential interfering radical−radical reactions such as the $C_6H_5O(\bullet) + C_6H_5O(\bullet)$, $C_6H_5O(\bullet)$ + Cl, and $C_6H_5O(\bullet)$ + F reactions. To check for such complications, experiments were performed using mixtures of 980 mbar of SF_6, 20 mbar of HCl, and 0.1 mbar of C_6H_5OH, with the maximum transient absorption at 235 nm measured as a function of radiolysis dose (and hence radical concentration). Figure 1 shows the observed maximum absorbance as a function of the dose. As seen from Figure 1, the absorption observed in experiments using maximum dose was significantly less than that expected on the basis of a linear extrapolation of the low-dose data. This observation suggests that unwanted radical−radical reactions become important at high radical concentrations.

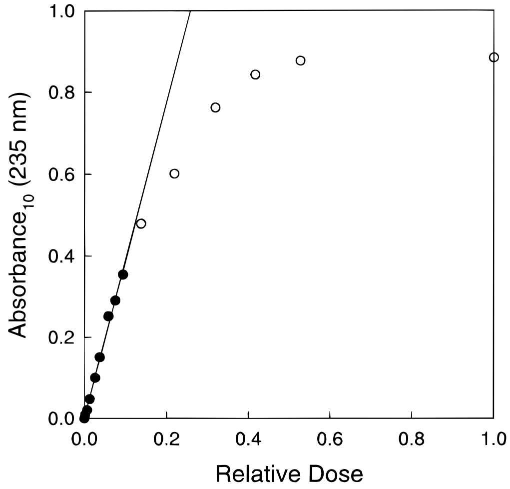

Figure 1. Maximum transient absorbance at 235 nm following the pulsed radiolysis of mixtures of 0.1 mbar C_6H_5OH, 20 mbar Cl_2, and 980 mbar SF_6 versus the radiolysis dose. The UV path length was 80 cm. The solid line is a linear regression of the low-dose data (filled circles).

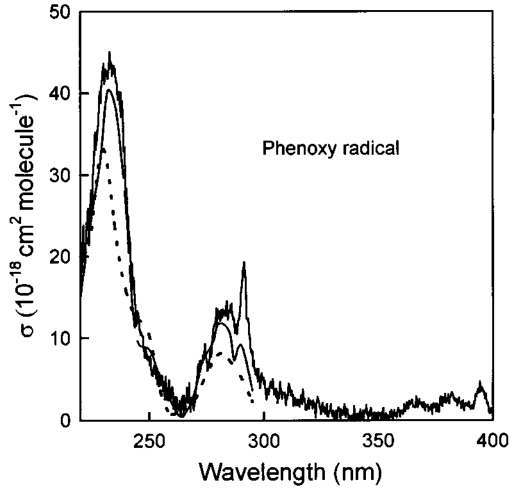

Figure 2. UV absorption spectra of $C_6H_5O(\bullet)$ radical measured in the present work (solid), by Berho et al.[6] (dashed), and by Kajii et al.[14] (dotted).

The line in Figure 1 is a linear least-squares fit to the low-dose data and has a slope of 3.88 ± 0.21. Combining this slope with the F atom yield of $(2.98 \pm 0.34) \times 10^{15}$ molecules cm^{-3} (full dose and $[SF_6] = 1000$ mbar) gives $\sigma_{235\ nm}(C_6H_5O(\bullet)) = (3.82 \pm 0.48) \times 10^{-17}$ cm^2 $molecule^{-1}$. The quoted uncertainty includes both statistical and potential systematic uncertainties and so reflects the accuracy of the measurement.

The spectrum of the phenoxy radical was measured by recording the initial absorbance following pulsed radiolysis of $SF_6/HCl/C_6H_5OH$ mixtures using the diode array. The delay was 0.6 μs and the integration time was 4 μs. The spectrum was placed on an absolute basis using $\sigma_{235\ nm} = 3.82 \times 10^{-17}$ cm^2 $molecule^{-1}$. The result is given in Figure 2 and Table 1. As seen from Figure 2, there is good agreement between the present result and the gas-phase spectra reported by Kajii et al.[14] and Berho and Lesclaux.[5] Interestingly, Schuler and Buzzard obtained a phenoxy spectrum by pulse radiolysis of N_2O-saturated aqueous solutions of C_6H_5OH,[15] which has the same characteristic fine structure around 395 nm as the present spectrum. Very recently Sehested[16] has obtained a phenoxy spectrum in the aqueous phase in the UV region, and the spectral features are indistinguishable from those found in the present gas-phase spectrum.

3.2. Kinetics of the Reaction of Phenoxy Radicals with NO and NO_2. The kinetics of the reactions of phenoxy radicals

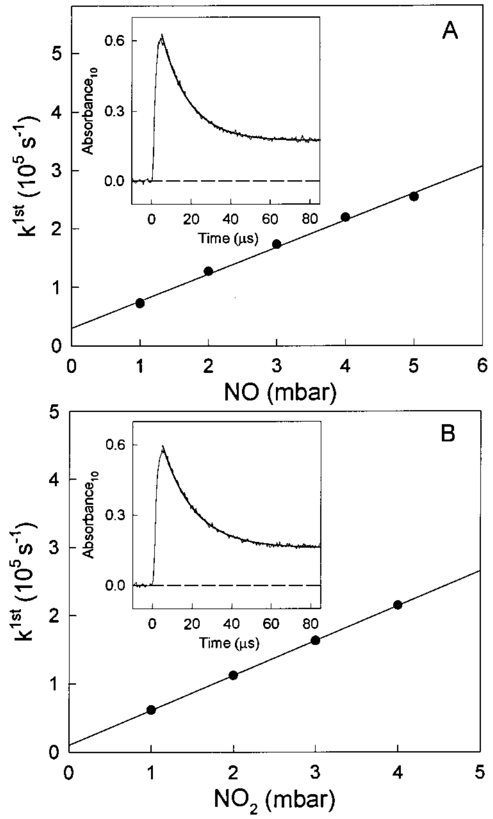

Figure 3. (A) Pseudo-first-order rate constants for reaction of $C_6H_5O(\bullet)$ radicals with NO following pulsed radiolysis of $SF_6/HCl/C_6H_5OH/NO$ mixtures versus [NO]. (B) Pseudo-first-order rate constants for reaction of $C_6H_5O(\bullet)$ radicals with NO_2 following pulsed radiolysis of $SF_6/HCl/C_6H_5OH/NO_2$ mixtures versus [NO_2]. The insets show first-order fits to transients at 235 nm observed following pulsed radiolysis (dose = 22% of maximum) of mixtures containing of 0.1 mbar C_6H_5OH, 20 mbar HCl, 980 mbar SF_6, and 1.0 mbar of either NO (A) or NO_2 (B).

TABLE 1: UV Absorption Cross Sections for $C_6H_5O(\bullet)$ Radicals

wavelength (nm)	$\sigma(C_6H_5O(\bullet))$ (10^{-18} cm^2 $molecule^{-1}$)	wavelength (nm)	$\sigma(C_6H_5O(\bullet))$ (10^{-18} cm^2 $molecule^{-1}$)
230	38.7	270	3.3
235	38.2	275	6.4
240	25.2	280	11.5
245	11.0	285	12.0
250	6.3	290	14.2
255	4.9	295	6.6
260	3.6	300	3.9
265	2.7		

with NO and NO_2 were studied by monitoring the decay in absorption at 235 nm (attributed to phenoxy radicals) following the radiolysis of $SF_6/HCl/C_6H_5OH/NO$ and $SF_6/HCl/C_6H_5OH/NO_2$ mixtures. The rate of decay of the absorbance at 235 nm increased linearly with the NO/NO_2 concentration. It seems reasonable to ascribe the decay of absorbance to loss of phenoxy radicals via reaction with NO/NO_2. The smooth curves in the insets in Figure 3A,B are first-order fits, which give pseudo-first-order rate constants, k^{1st}, of 7.20×10^4 and 6.14×10^4 s^{-1}, respectively. We ascribe the residual absorption in the inserts to UV absorption by C_6H_5ONO and $C_6H_5ONO_2$. While there are no reported measurements of the UV absorption spectrum of $C_6H_5ONO_2$, Berho et al.[6] have reported $\sigma(C_6H_5ONO) = 5.0 \times 10^{-18}$ cm^2 $molecule^{-1}$ at 240 nm. From the inset in Figure 3A, it can be seen that the residual absorption at 235 nm that we attribute to C_6H_5ONO is approximately a factor of 4 less than that of $C_6H_5O(\bullet)$. Using $\sigma(C_6H_5O(\bullet)) = 3.8 \times 10^{-17}$ (Table 1), we arrive at an estimate of $\sigma(C_6H_5ONO) = 1.0 \times 10^{-17}$ cm^2 $molecule^{-1}$ at 235 nm. This result is a factor of 2 greater than that reported by Berho et al.[6] at 240 nm, which presumably reflects an increase in UV absorption by C_6H_5ONO from 240 to 235 nm. All experimental traces followed pseudo-first-order kinetics. To allow for sufficient time for conversion of F atoms into Cl atoms and subsequently into phenoxy radicals, the analysis of the decay traces was initiated 5 µs after the radiolysis pulse. The pseudo-first-order loss rates for $C_6H_5O(\bullet)$ radicals in the presence of NO_x are plotted versus the concentrations of NO and NO_2 in Figure 3. Linear least-squares analysis gives $k_3 = (1.88 \pm 0.16) \times 10^{-12}$ and $k_4 = (2.08 \pm 0.15) \times 10^{-12}$ cm^3 $molecule^{-1}$ s^{-1}. The small positive y-axis intercepts in Figure 3A,B may reflect the contribution of self-reaction to loss of $C_6H_5O(\bullet)$ radicals. These small intercepts do not impact the measured values of k_3 and k_4. Our kinetic data for reaction 3 are in excellent agreement with the measurement of $k_3 = 1.7 \times 10^{-12}$ cm^3 $molecule^{-1}$ s^{-1} by Berho and Lesclaux.[6] There are no literature data for k_4 to compare with our results.

3.3. The Reaction of Cl_2 with C_6H_5OH. In the smog chamber studies, $C_6H_5O(\bullet)$ radicals were generated by UV irradiation of C_6H_5OH/Cl_2 mixtures in 700 Torr of N_2, air, or O_2 diluent. Prior to such studies, experiments were performed to characterize this source of $C_6H_5O(\bullet)$ radicals in the FTIR smog chamber system. Control experiments were performed to test for unwanted loss of C_6H_5OH via deposition to the chamber walls, photolysis, or reaction with molecular chlorine. In the first experiment a mixture of 9 mTorr of C_6H_5OH in 700 Torr of N_2 was introduced into the chamber and monitored for 1 h. During the first 30 min there was a small but noticeable (~5%) loss of C_6H_5OH presumably reflecting deposition to the walls. In the subsequent 30 min there was no additional loss of C_6H_5OH presumably reflecting saturation of the walls with C_6H_5OH. UV irradiation for 1 min produced no discernible loss of C_6H_5OH, showing that photolysis of C_6H_5OH is not important. Interestingly, when C_6H_5OH/Cl_2 mixtures in N_2 or O_2 diluent were introduced into the chamber and allowed to stand in the dark for 15−55 min a substantial (up to 80%) and continual loss of C_6H_5OH was observed. We ascribe this loss of C_6H_5OH to homogeneous and/or heterogeneous reaction with Cl_2.

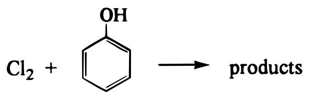

(8)

To study the rate of reaction 8, mixtures of 3.0−8.8 mTorr of C_6H_5OH and 0−1.2 Torr of Cl_2 in 700 Torr of N_2 or O_2 diluent were prepared, and the loss of C_6H_5OH was monitored. As shown in Figure 4A, in all experiments the observed loss of C_6H_5OH followed first-order kinetics. Linear least-squares fits to the data in Figure 4A give pseudo-first-order rate constants, k^{1st}, which are plotted versus [Cl_2] as the circles in Figure 5, linear least-squares analysis gives $k_8 = (1.8 \pm 0.1) \times 10^{-20}$ cm^3 $molecule^{-1}$ s^{-1}. It is unclear whether the reaction of C_6H_5OH with Cl_2 occurs via a homogeneous or heterogeneous mechanism. To provide insight into this question, additional experiments were performed using a small (25 L) reaction chamber, which has a surface area to volume ratio approximately three times that of the large chamber. Experiments in the small chamber employed mixtures of 30−35 mTorr of C_6H_5OH and 0−100 mTorr of Cl_2 in 700 Torr of N_2. The results are shown

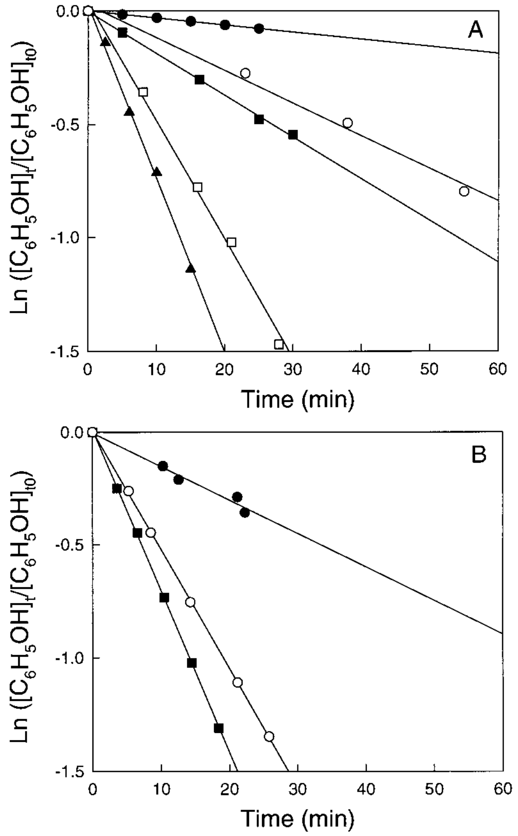

Figure 4. Loss of C_6H_5OH when C_6H_5OH/Cl_2 mixtures were allowed to stand in the dark in the 140 (A) or 25 L (B) chambers. The Cl_2 concentrations (in units of mTorr) were (A) 28.1 (●), 299 (○), 714 (■), 1200 (□), and 1840 (▲); (B) 0.0 (●), 50 (○), and 100 (■). All experiments were performed in 700 Torr total pressure of N_2 diluent at 296 K.

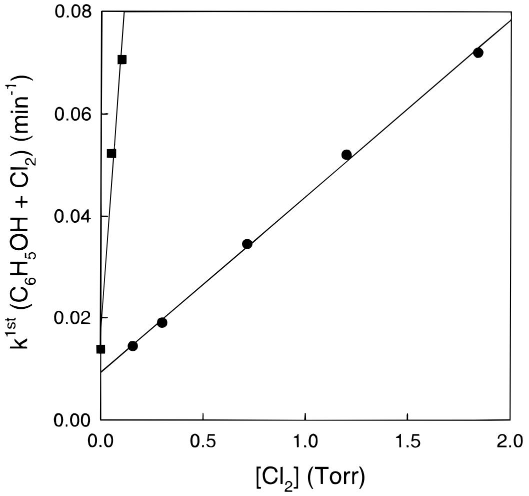

Figure 5. Pseudo-first-order loss rate of C_6H_5OH versus $[Cl_2]$ observed in the large (●) and small (■) chambers.

in Figure 4B, and the corresponding k^{1st} values are indicated by the squares in Figure 5. It is clear from Figure 5 that the reaction of C_6H_5OH with Cl_2 proceeds more rapidly in the small reaction chamber. We conclude that the reaction in the small chamber has a significant heterogeneous component. We are unable to exclude a significant heterogeneous component to the reaction observed in the large chamber, and consequently we choose to quote an upper limit of $k_8 < 1.9 \times 10^{-20}$ cm^3 molecule^{-1} s^{-1} for the gas-phase reaction of C_6H_5OH with Cl_2 at 296 K.

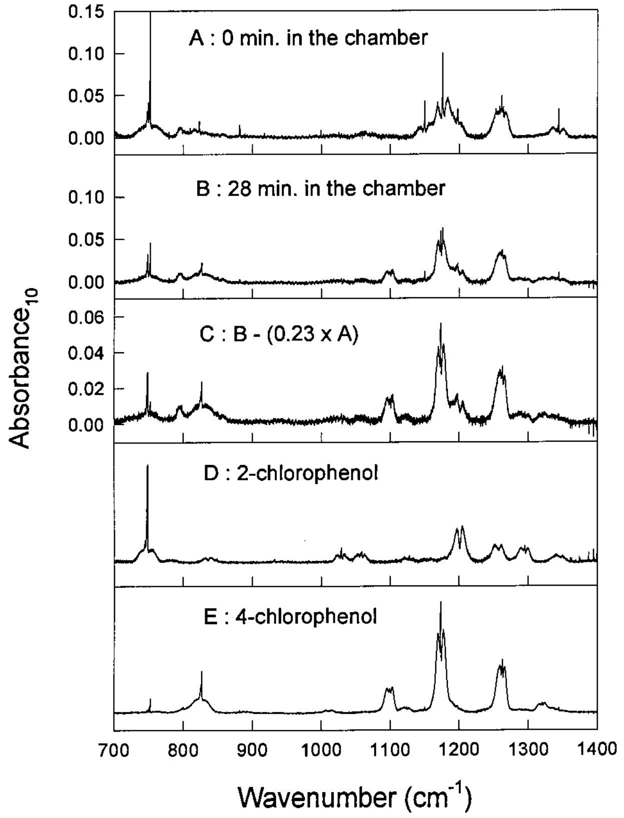

Figure 6. IR spectra acquired before (A) and after (B) a mixture of 2.2 mTorr of C_6H_5OH and 1.2 Torr of Cl_2 in 700 Torr total pressure of N_2 diluent was allowed to stand in the dark for 28 min; 77% of the C_6H_5OH was consumed. Subtraction of features attributable to C_6H_5-OH from panel B gives panel C. Reference spectra of 2- and 4-chlorophenol are given in panels D and E.

The products resulting from the reaction between Cl_2 and C_6H_5OH were identified using FT-IR spectroscopy.

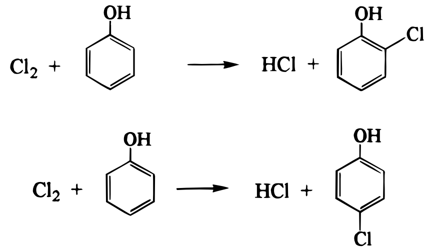

(8a)

(8b)

Figure 6 shows IR spectra acquired immediately after a mixture of 2.2 mTorr of C_6H_5OH and 1.2 Torr of Cl_2 in 700 Torr of N_2 diluent was introduced into the 140 L chamber (A) and 28 min later (B). Subtraction of features attributable to C_6H_5OH from panel B gives panel C. Comparison with reference spectra of 2- and 4-chlorophenol (panels D and E) shows the formation of these products. After subtraction of IR features attributable to 2- and 4-chlorophenol, there were trace features that were identified as belonging to 2,4-dichlorophenol. No other features were observed.

Figure 7 shows the observed formation of 2- and 4-chlorophenol when C_6H_5OH/Cl_2 mixtures in 700 Torr of N_2 or O_2 diluent were allowed to stand in the dark. Linear least-squares analysis gives yields of (28 ± 3)% for 2-chlorophenol and (75 ± 4)% for 4-chlorophenol. The combined yields of 2- and 4-chlorophenol account for 100% of the C_6H_5OH loss, and we conclude that $k_{8a}/k_8 = 0.28 \pm 0.03$ and $k_{8b}/k_8 = 0.75 \pm 0.04$.

3.4. Kinetics of the Reactions of Cl with C_6H_5OH, Benzoquinone, and 2-, 3-, and 4-Chlorophenol. Relative rate

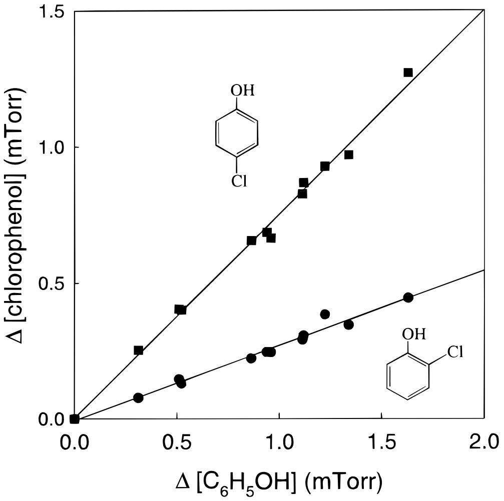

Figure 7. Formation of 2-chlorophenol (●) and 4-chlorophenol (■) versus loss of C_6H_5OH due to reaction between Cl_2 and C_6H_5OH. The yields of 2- and 4-chlorophenol were (28 ± 3)% and (75 ± 4)%, respectively.

techniques were used to investigate the reactivity of Cl atoms toward C_6H_5OH, benzoquinone, and 2-, 3-, and 4-chlorophenol. The techniques used have been described previously.[17] Photolysis of Cl_2 was the source of Cl atoms.

$$Cl_2 \xrightarrow{h\nu} 2\ Cl \qquad (9)$$

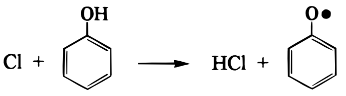

(1)

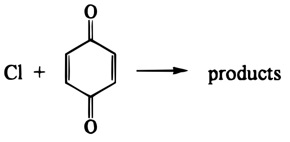

(10)

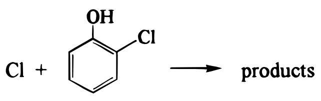

(11)

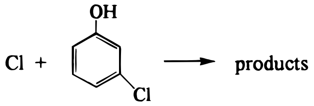

(12)

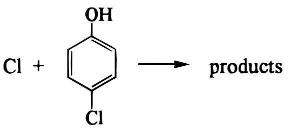

(13)

The kinetics of reactions 1, 10, 11, 12, and 13 were measured relative to reactions 14−17.

$$Cl + C_2H_4 \longrightarrow \text{products} \qquad (14)$$

$$Cl + C_3H_6 \longrightarrow \text{products} \qquad (15)$$

$$Cl + CH_3OCH_3 \longrightarrow \text{products} \qquad (16)$$

$$Cl + C_2H_5Cl \longrightarrow \text{products} \qquad (17)$$

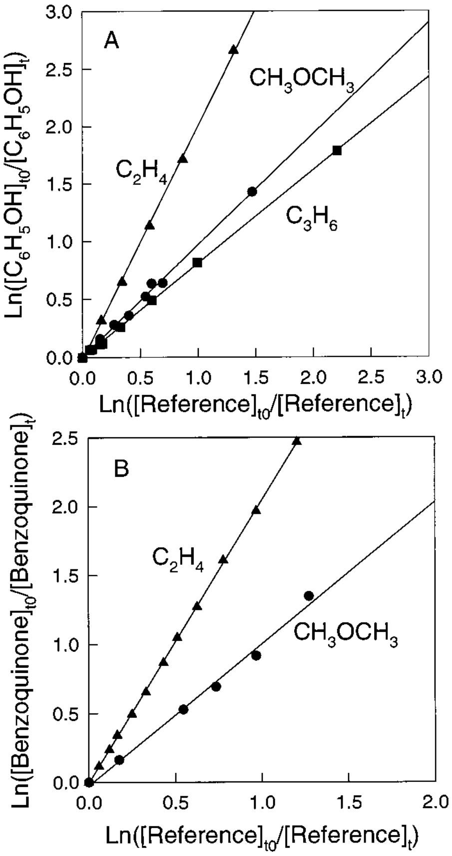

Figure 8. (A) Decay of C_6H_5OH versus C_2H_4 (▲), CH_3OCH_3 (●), and C_3H_6 (■) and (B) benzoquinone versus C_2H_4 (▲) and CH_3OCH_3 (●) when mixtures of these compounds were exposed to Cl atoms in 700 Torr total pressure of N_2 at 296 K.

Control experiments were performed to check for complications caused by photolysis, heterogeneous loss, and reaction of Cl_2 with benzoquinone and 2-, 3-, and 4-chlorophenol; no evidence for such complications was observed. As discussed in the previous section, reaction of molecular chlorine with phenol is significant and needs to be taken into account. The experimental conditions used in the study of reaction 1 were $[Cl_2] = 28$ mTorr, $[C_6H_5OH] = 6$ mTorr, and [Reference] = 7.4−17 mTorr. From Figure 5 it can be seen that for $[Cl_2] = 28$ mTorr the pseudo-first-order loss rate of C_6H_5OH with respect to reaction 8 is 9×10^{-3} min^{-1}. This pseudo-first-order rate constant was used to compute corrections for loss of C_6H_5OH via reaction 8. The corrections were always less than 10% of the overall loss of C_6H_5OH in the relative rate experiments. The observed loss of C_6H_5OH (corrected for reaction 8) and the reference compounds when reaction mixtures were exposed to Cl atoms is shown in Figure 8A. Results for benzoquinone and 2-, 3-, and 4-chlorophenol are shown in Figures 8B and 9. Experiments were performed in 700 Torr of either N_2 or air. There was no discernible effect of the diluent gas.

Rate constant ratios obtained by linear least-squares analysis of the data in Figures 8 and 9 are given in Table 2. Using $k_{14} = 9.4 \times 10^{-11}$,[18] $k_{15} = 2.56 \times 10^{-10}$,[19] $k_{16} = 1.9 \times 10^{-10}$,[20] and $k_{17} = 8.0 \times 10^{-12}$ [21] gives the values of k_1, k_{10}, k_{11}, k_{12}, and k_{13} listed in Table 3. Consistent kinetic data was obtained using the different reference reactions indicating the absence of unwanted secondary reactions. We choose to quote values for k_1, k_{10}, k_{11}, k_{12}, and k_{13} that are the averages of the results given in Table 3 with error limits that encompass the extremes of the individual determinations; hence, $k_1 = (1.93 \pm 0.29) \times 10^{-10}$, $k_{10} = (1.94 \pm 0.28) \times 10^{-10}$, $k_{11} = (7.32 \pm 1.08) \times 10^{-12}$, $k_{12} = (1.56 \pm 0.14) \times 10^{-10}$, and $k_{13} = (2.37 \pm 0.21) \times 10^{-10}$ cm^3 molecule^{-1} s^{-1}. We estimate that potential systematic

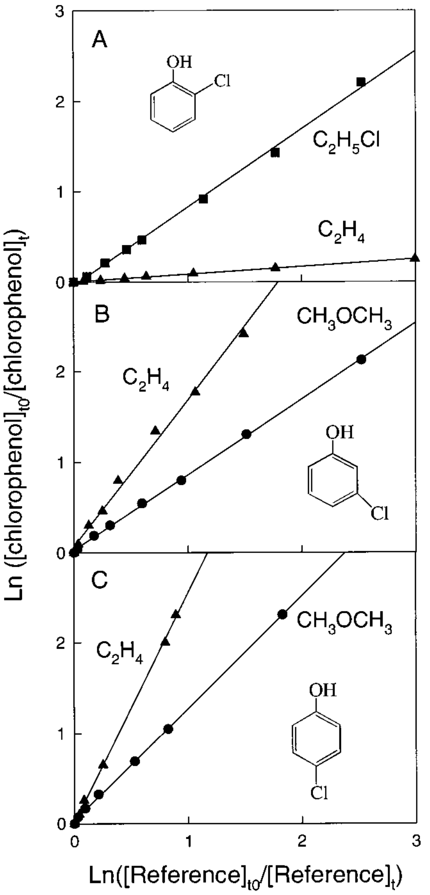

Figure 9. (A) Decay of 2-chlorophenol versus C_2H_5Cl (■) and C_2H_4 (▲), (B) 3-chlorophenol and (C) 4-chlorophenol versus C_2H_4 (▲) and CH_3OCH_3 (●) when mixtures of these compounds were exposed to Cl atoms in 700 Torr total pressure at 296 K.

TABLE 2: Rate Constant Ratios, *k*(Cl + Reactant)/*k*(Cl + Reference), Measured in 700 Torr of N_2/Air Diluent at 296 K

	reference			
reactant	C_2H_4	C_3H_6	CH_3OCH_3	C_2H_5Cl
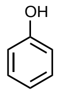	2.03 ± 0.14	0.81 ± 0.06	0.97 ± 0.07	
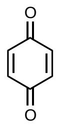	2.05 ± 0.02		1.03 ± 0.09	
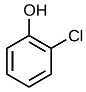	8.26 ± 0.58			0.86 ± 0.08
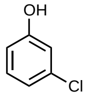	1.62 ± 0.12		0.83 ± 0.06	
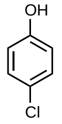	2.53 ± 0.21		1.24 ± 0.10	

TABLE 3: Rate Constants *k*(Cl + Reactant) Measured Using Various Reference Compounds (Units Are 10^{-10} cm^3 molecule^{-1} s^{-1})

	reference			
reactant	C_2H_4	C_3H_6	CH_3OCH_3	C_2H_5Cl
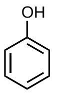	1.91 ± 0.13 1.91 ± 0.23	2.07 ± 0.15	1.84 ± 0.13 1.96 ± 0.26	
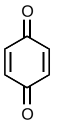	0.078 ± 0.005			0.069 ± 0.006
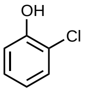	1.53 ± 0.11		1.58 ± 0.11	
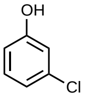	2.37 ± 0.19		2.36 ± 0.20	

errors associated with uncertainties in the reference rate constants could add an additional 10% to the uncertainty range. Propagating this additional uncertainty gives final values of $k_1 = (1.93 \pm 0.36) \times 10^{-10}$, $k_{10} = (1.94 \pm 0.35) \times 10^{-10}$, $k_{11} = (7.32 \pm 1.30) \times 10^{-12}$, $k_{12} = (1.56 \pm 0.21) \times 10^{-10}$, and $k_{13} = (2.37 \pm 0.30) \times 10^{-10}$ cm^3 molecule^{-1} s^{-1}.

Our value of $k_1 = (1.93 \pm 0.36) \times 10^{-10}$ is consistent with that of $k_1 = (2.4 \pm 0.4) \times 10^{-10}$ cm^3 molecule^{-1} s^{-1} by Buth et al.[14] The rate constants for the reactions between Cl atoms and C_6H_5OH, benzoquinone, and 3- and 4-chlorophenol are all close to the gas kinetic limit. In contrast, the reactivity of 2-chlorophenol toward Cl atoms is 30 times less than that of 3- and 4-chlorophenol. While there is significant intramolecular hydrogen bonding between the −OH and −Cl substituents in 2-chlorophenol,[22,23] the molecular geometry in 3- and 4-chlorophenol precludes such interaction. It seems likely that the additional stability conferred by intramolecular hydrogen bonding in 2-chlorophenol lowers its reactivity toward Cl atoms.

3.5. FT-IR Study of the Reaction of O_2 with $C_6H_5O(\bullet)$ Radical. It has been shown previously that the reaction between Cl atoms and C_6H_5OH, reaction 1, is a clean source of $C_6H_5O(\bullet)$ radicals.[14] The aim of the work described in this section was to provide information concerning the likely atmospheric fate of $C_6H_5O(\bullet)$ radicals.

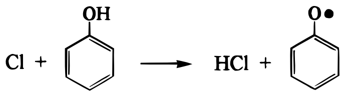

(1)

Experiments were performed using the UV irradiation of C_6H_5OH/Cl_2 mixtures in 700 Torr total pressure of N_2, air, or O_2 diluent at 296 K. Figure 10 shows spectra acquired before (A) and after (B) a 1 min irradiation of a mixture containing 5.5 mTorr of C_6H_5OH and 44 mTorr of Cl_2 in 700 Torr of O_2 diluent. Three products were observed: 2-chlorophenol, 4-chlorophenol, and an unknown product(s), which we will label "X", with IR features at 755, 844, 1210, 1488, and 1590 cm^{-1}. Subtraction of IR features attributed to C_6H_5OH, 2-chlorophenol, and 4-chlorophenol from panel B gives the spectrum of X displayed in panel C. The magnitudes of the yields of the chlorophenols were consistent with those expected from the "dark" reaction between molecular chlorine and C_6H_5OH discussed in section 3.3. The absorption features of X increased linearly with consumption of C_6H_5OH over the range 17−85% showing that this compound(s) is relatively unreactive toward Cl atoms.

The yield of X in experiments using 700 Torr of N_2, air, or O_2 diluents was indistinguishable. We conclude that formation of X does not involve O_2 and that even in the presence of 700 Torr of O_2 diluent, reaction 2 is unimportant.

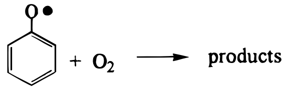

(2)

On the basis of the kinetic data for the phenoxy radical self-reaction reported by Berho and Lesclaux,[5] we estimate that the steady-state phenoxy radical concentration in the present experiments was of 10^{11} cm^{-3}, i.e., 8 orders of magnitude less than $[O_2]$. Given the huge excess of O_2, it is notable that no evidence for reaction between phenoxy and O_2 was observed. Clearly, the rate constant for reaction 2 is very small. To place an upper limit on k_2, the system was modeled using the Acuchem chemical kinetic program[24] with a mechanism in which reaction 2 competes with the self-reaction of phenoxy radicals with a rate constant 1.2×10^{-11} cm^3 molecule^{-1} s^{-1}.[5] From the observation that there was no discernible change (<10%) in the products observed in experiments performed in pure O_2 or N_2 diluents, we are able to establish an upper limit of $k_2 < 5.0 \times 10^{-21}$ cm^3 molecule^{-1} s^{-1} at 296 K.

3.6. FT-IR, Electronic Structure, and GC−MS Study of $C_6H_5O(\bullet)$ Radical Self-Reaction. Given that reaction with O_2 is unimportant, we need to consider a number of other possibilities for the source of the unknown compound(s) X in the smog chamber experiments:

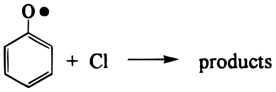

(18)

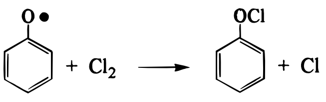

(19)

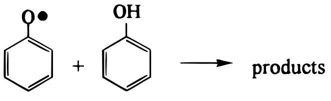

(20)

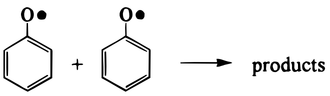

(21)

Reaction of Cl atoms with C_6H_5OH proceeds at a rate close to the gas kinetic limit (see section 3.4). For low consumptions (<20%) of C_6H_5OH, reaction 18 will not play any significant role, but the concentration of X was observed to increase linearly over the entire range of C_6H_5OH consumptions used (17−85%). We conclude that reaction 18 is not the source of X.

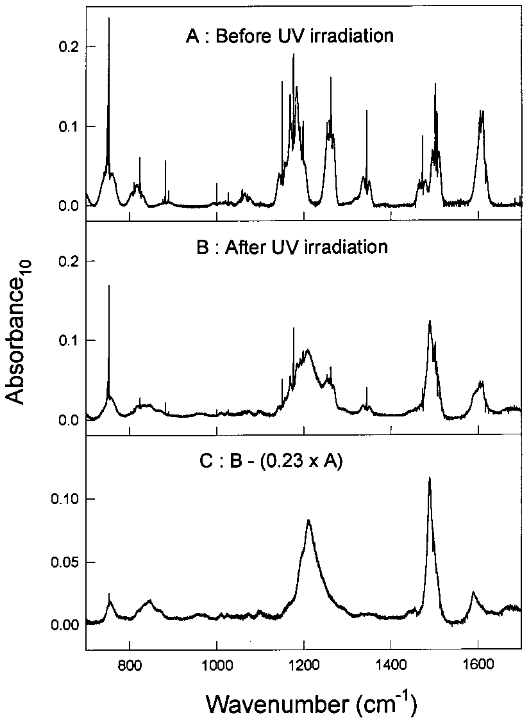

Figure 10. IR spectra acquired before (A) and after (B) a 60 s irradiation of a mixture of 5.5 mTorr of C_6H_5OH and 44 mTorr of Cl_2 in 700 Torr total pressure of O_2 diluent. During the irradiation 73% of the C_6H_5OH was consumed. Subtraction of features attributable to C_6H_5OH and chlorophenol from panel B gives panel C. We assign the IR features in panel C to the product of the self-reaction of $C_6H_5O(\bullet)$ radicals.

TABLE 4: Calculated Total Electronic Binding Energies[a] and Enthalpy Corrections to 298 K (kcal mol^{-1})

		LSDA	PW91	ZPE + 298 K
Cl	^2P	−4.5	−4.9	0.9
Cl_2	$D_{\infty h}$	−81.7	−72.2	2.4
$C_6H_5O(\bullet)$	C_{2v} ($^2B_2$)	−1896.5	−1782.9	59.2
C_6H_5OH	C_s	−2020.3	−1897.9	65.7
C_6H_5OCl	C_s	−1944.7	−1816.7	59.9
$C_6H_5OOC_6H_5$	C_2	−3814.0	−3566.5	121.4
4-$C_6H_5OC_6H_4OH$	C_1	−3870.7	−3618.9	120.3
4,4′-$HOC_6H_4C_6H_4OH$	C_2	−3883.0	−3620.5	120.3
$CH_3O(\bullet)$	C_s ($^2A'$)	−586.8	−564.5	23.1
CH_3OOCH_3	C_2	−1233.2	−1170.3	53.3

[a] Binding energies reported with respect to spin-restricted atoms.

To establish whether X could be the phenyl hypochlorite (C_6H_5OCl) formed via reaction of $C_6H_5O(\bullet)$ radicals with Cl_2, we used electronic structure calculations to estimate the thermodynamics of reaction 19. The calculated (PW91) structures of $C_6H_5O(\bullet)$ and C_6H_5OCl are shown in Figure 11, and the energies of these species and of $Cl(\bullet)$ and Cl_2 reported in Table 4. Direct evaluation of the reaction energy at this level of theory is expected to be reliable to within ±5 kcal mol^{-1}. We calculate reaction 19 to be endothermic by 32 kcal mol^{-1} at 298 K. Taking the heats of formation of $C_6H_5O(\bullet)$ and $Cl(\bullet)$ to be 11.4[25] and 29.0 kcal mol^{-1},[26] respectively, implies a heat of formation of C_6H_5OCl of about 14 kcal mol^{-1}. Given the highly unfavorable thermodynamics of reaction 19, we conclude that it is unimportant in our system and X is not C_6H_5OCl.

The product(s) X must arise, then, from either the self-reaction of $C_6H_5O(\bullet)$ radicals or their reaction with C_6H_5OH. It is unlikely that these two pathways can be distinguished on the basis of the identity of X. Two other pieces of evidence argue against reaction 20, however. First, Berho and Lesclaux have reported the results of a study of the kinetics of the $C_6H_5O(\bullet)$ radical self-reaction in the presence of 3−12 mTorr of phenol.[15] The loss of $C_6H_5O(\bullet)$ radicals followed second-order kinetics and was insensitive to variation of the phenol concentration suggesting reaction 20 is of negligible importance. Second, Buth et al.[4] monitored the loss of phenol in the presence of Cl atoms in a discharge flow study of k_1. Variation of the initial phenol concentration over the range 0.2−3.7 mTorr had no discernible impact on the measured value of k_1, suggesting, but not proving, that reaction 20 is not significant.

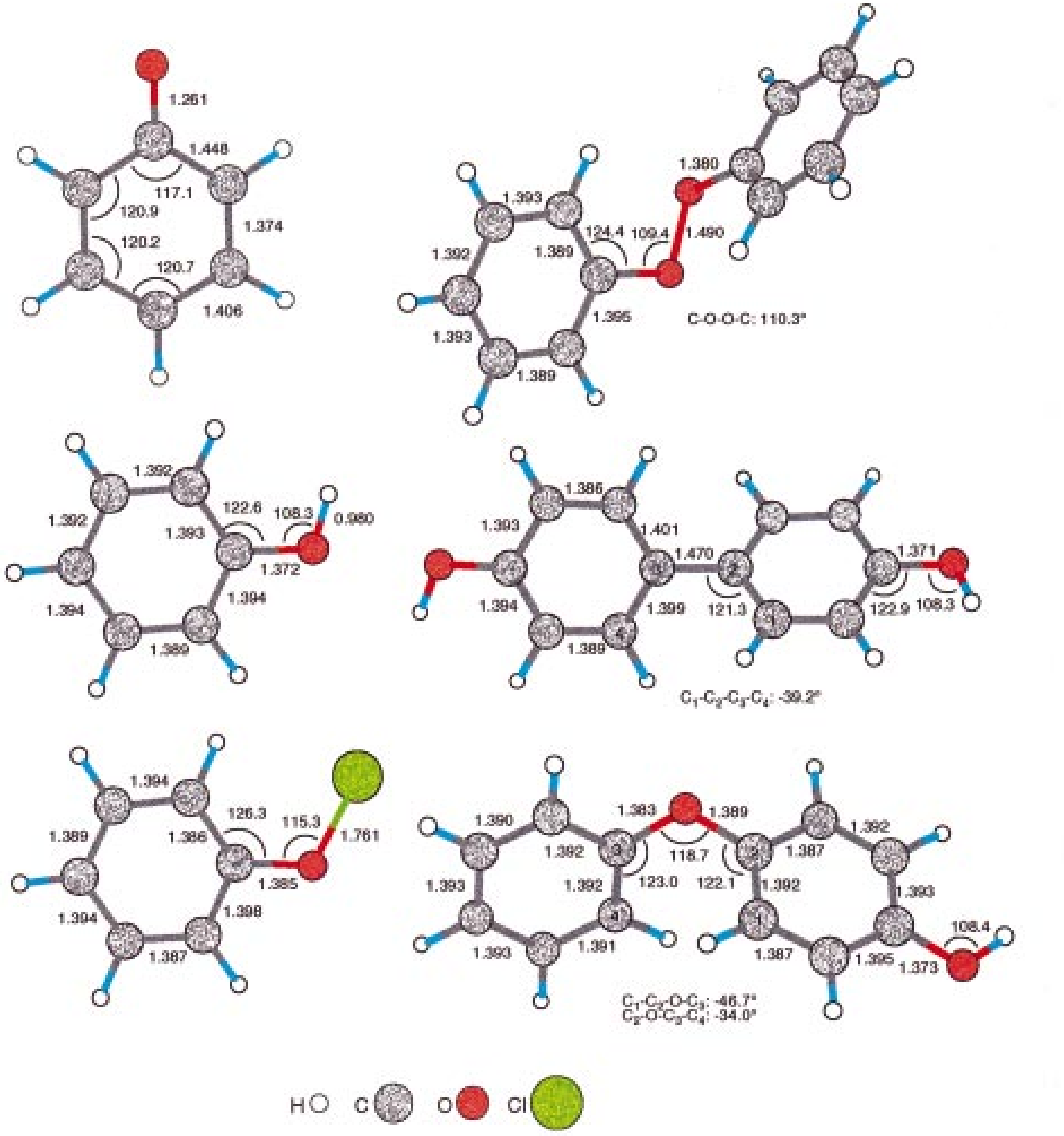

Figure 11. PW91 calculated structures.

It is most likely, then, that the product(s) X arise from the self-reaction of phenoxy radicals. In considering the possible products of reaction 21, we note that the electronic structure of $C_6H_5O(\bullet)$ radicals can be represented as an admixture of three principle resonance structures, which are expected to dominate in determining self-reaction products.

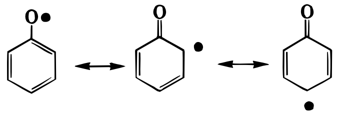

While intuitively the first resonance structure might be expected to dominate, in fact density functional calculations predict Mulliken spin densities of 0.40, 0.27, and 0.36 electrons at the phenoxy oxygen, ortho, and para carbon positions, respectively. In contrast, the meta position has a Mulliken spin density of only −0.10 electrons. Consistent with this description, the phenoxy C−O bond length is only 1.261 Å, compared to 1.372 Å in phenol, reflecting the partial C═O character, and the C_6 ring exhibits a pronounced bond alternation (Figure 11). If we assume the most probable products of self-reaction to be those arising from dimerization of the phenoxy radical at these radical centers, then 3! = 6 products are possible, which are shown below. It seems most likely that X is one, or some combination, of these six species.

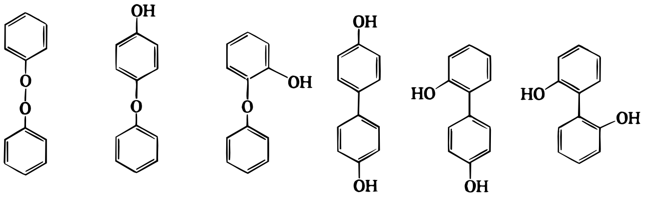

We used density functional theory to investigate the structures, energetics, and vibrational spectra of the diphenyl peroxide and a representative ether (4-phenoxyphenol) and biphenyl (4,4′-biphenol). The LDA structures are shown in Figure 11. Figure 12 contains calculated (LDA) vibrational spectra for these three isomers, with the bands artificially broadened using a Lorentzian distribution with a peak width at half-height of 10 cm^{-1}. The calculated spectra tend to overestimate peak locations by several percent but otherwise agree well with literature spectra of 4-phenoxyphenol and 4,4′-biphenol.[27] The LDA vibrational frequencies shown in Figure 12 are scaled by 0.97 to account for this systematic overestimation. The results illustrate the difficulty in identifying the products of phenoxy radical self-reaction on the basis of vibrational spectroscopy. All three isomers (and by inference, the three isomers we have not examined) are predicted to exhibit four principle features in their vibrational spectrum in the region of interest, at 1570−1605 cm^{-1} (ring e_{2g} deformation), 1430−1474 cm^{-1} (e_{1u} C−H bending), 1193−1253 cm^{-1} (C−O stretches), and 1110−1120 cm^{-1} (e_{2g} C−H bending and OH bending). The experimental spectrum of the unknown product(s) X is consistent with these predictions, but the observed bands are broad and featureless. It is not possible to identify X on the basis of its vibrational spectrum, except to conclude that it likely includes some combination of the six self-reaction products suggested above.

We also examined the energetics of formation of the three phenoxy radical dimers, using the PW91 energies and corrections to 298 K reported in Table 4:

$$2C_6H_5O(\bullet) \rightarrow C_6H_5OOC_6H_5 \qquad \Delta H^\circ_{298} = +2.2 \text{ kcal mol}^{-1} \quad (22)$$

$$2C_6H_5O(\bullet) \rightarrow 4\text{-}C_6H_5OC_6H_4OH \qquad \Delta H^\circ_{298} = -51.3 \text{ kcal mol}^{-1} \quad (23)$$

$$2C_6H_5O(\bullet) \rightarrow 4,4'\text{-}HOC_6H_4C_6H_4OH \qquad \Delta H^\circ_{298} = -60.6 \text{ kcal mol}^{-1} \quad (24)$$

Formations of both the ether and biphenyl are substantially exothermic and equally likely on thermodynamic grounds. Combined with the heat of formation of $C_6H_5O(\bullet)$,[26] we obtain −28 and −38 kcal mol^{-1} for the heats of formation of 4-$C_6H_5OC_6H_4OH$ and 4,4′-$HOC_6H_4C_6H_4OH$, respectively. We expect the other ether and biphenyl isomers to have similar energetics. In contrast, formation of the peroxide is predicted to be slightly endothermic from the direct calculation. To check this result, we calculated the energy of the following isodesmic reaction:

$$2C_6H_5O(\bullet) + CH_3OOCH_3 \rightarrow C_6H_5OOC_6H_5 + 2CH_3O(\bullet) \qquad \Delta H^\circ_{298} = -60.6 \text{ kcal mol}^{-1}$$

Combining this reaction enthalpy with the known $CH_3O{-}OCH_3$ bond strength (37.6 kcal mol^{-1} [25], we obtain $\Delta H^\circ_{298} = +1.2$ kcal mol^{-1} for reaction 22. While the density functional approach used here may somewhat overestimate the enthalpy of reaction 22, we do not expect $C_6H_5OOC_6H_5$ to be a thermodynamically stable product of phenoxy radical self-reaction and do not expect it to comprise a significant fraction of X.

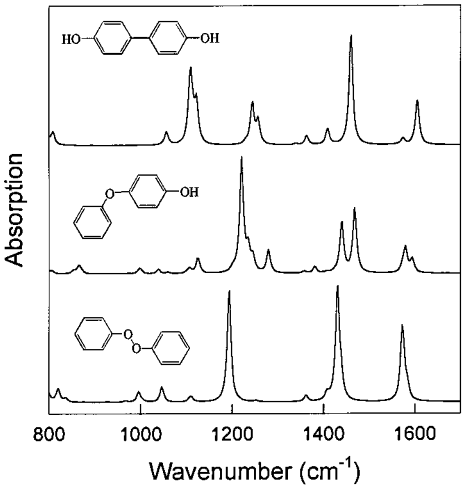

Figure 12. LSDA calculated vibrational spectra of three possible products of phenoxy radical self-reaction. Frequencies scaled by 0.97, and bands artificially broadened by 10 cm^{-1}.

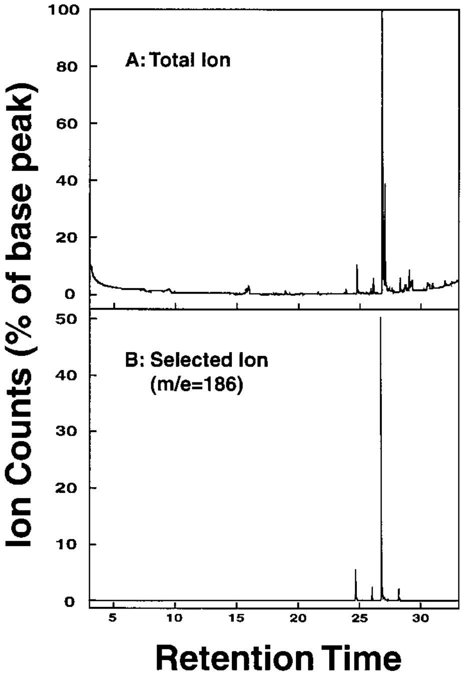

Figure 13. Total (A) and selected (B) ion chromatograms of the products following UV irradiation of a $C_6H_5OH/Cl_2/N_2$ mixture (see text for details).

The FT-IR and computational results provide some insight into the likely composition of the unknown X. To provide further information the product mixtures were analyzed using a GC−MS technique. Samples were collected by pumping the reaction mixtures out of the chamber slowly through a glass trap maintained at 0 °C using an ice bath. The resulting sample was dissolved in 0.5 cm^3 of CH_2Cl_2, and 1 μL aliquots were then injected onto the column of the GC−MS instrument. The top panel in Figure 13 shows the total ion chromatogram of the reaction products observed following a 95 s irradiation of a mixture of 14.8 mTorr of C_6H_5OH and 30 mTorr of Cl_2 in 700 Torr of N_2. The consumption of C_6H_5OH in this experiment was 37% (measured using the FT-IR system). The $(C_6H_5O)_2$

isomers have a molecular weight of 186 mass units. The bottom panel in Figure 13 shows the contribution of ions of mass 186 to the total ion chromatogram. As seen from Figure 13 ions of mass 186 make a major contribution to the total ion chromatogram. The second largest peak in panel A, which elutes at 27 min, 7 s has a mass of 220 and a fragmentation pattern consistent with its identification as a monochlorinated product ($C_{12}H_9$-ClO_2). We believe it likely that chlorination occurs as the sample is condensed in the cold trap. The fragmentation pattern of each 186 mass ion showed a loss of the following three fragments: a 17 mass fragment (OH), a 28 mass fragment (CO), and a 29 mass fragment (CHO). These fragments are expected from phenolic compounds[28] and are consistent with the formation of the $(C_6H_5O)_2$ dimer. Authentic reference samples of 2,2′-biphenol, 4,4′-biphenol, and 4-phenoxyphenol were available, and the response of the GC−MS system was tested for these compounds. From its retention time and fragmentation pattern the largest 186 mass product peak (see Figure) was identified as 4-phenoxy phenol. The other three peaks were not identified. The results obtained using the GC−MS system are entirely consistent with the conclusions based on the analysis above that the major fate of phenoxy radicals in our experiments is self-reaction.

4. Conclusions

We present here a large body of data concerning the atmospheric fate of phenoxy radicals. The reaction of phenoxy radicals with O_2 is extremely slow, and an upper limit of $k_2 < 5 \times 10^{-21}$ cm^3 molecule^{-1} s^{-1} at 296 K is reported. This result is consistent with the upper limit of $k_2 < 2 \times 10^{-18}$ cm^3 molecule^{-1} s^{-1} at temperatures up to 500 K reported by Berho and Lesclaux.[5] In contrast to their behavior toward O_2, phenoxy radicals react rapidly with NO and NO_2 with rate constants of $(1.88 \pm 0.16) \times 10^{-12}$ and $(2.08 \pm 0.15) \times 10^{-12}$ cm^3 molecule^{-1} s^{-1} at 296 K. Our result for k_3 is in good agreement with the recent measurement by Berho et al.[6] of $k_3 = (1.7 \pm 0.1) \times 10^{-12}$ cm^3 molecule^{-1} s^{-1} at 293 K. In moderately polluted urban atmospheres the concentration of NO_x ($NO + NO_2$) is typically 1−10 ppb, i.e., 10^8−10^7 times less than that of O_2. From the present work we conclude that phenoxy radicals react at least 4×10^8 times more rapidly with NO_x than with O_2. It then follows that under conditions typical of moderately polluted urban air, reaction of phenoxy radicals with O_2 is not important. It seems likely that the fate of phenoxy radicals in such environments will be reaction with NO_x, which will presumably lead to the formation of nitroso- and nitrophenols, thereby sequestering NO_x and slowing down the reactions responsible for ozone formation. This conclusion is consistent with the large negative incremental reactivity (ozone-forming potential) of benzaldehyde, which has been observed in smog chamber experiments.[29] Further work is needed to establish the products of the reaction of phenoxy radicals with NO_x and to investigate whether other species (for example, ozone) compete with NO_x for the phenoxy radicals.

Acknowledgment. We thank Robert Lesclaux (Université Bordeaux) for preprints of refs 5 and 6. The work conducted at Risø was funded by the European Union and Ford Forschungszentrum Aachen.

References and Notes

(1) *Motor Gasoline*; Marshall, Owen, Eds.; Royal Society of Chemistry.

(2) Seinfeld, J. H.; Pandis, S. N. *Atmospheric Chemistry and Physics*; John Wiley & Sons, Inc.: New York, 1998.

(3) Odum, J. R.; Jungkamp, T. P. W.; Griffin, R. J.; Flagan, R. C.; Seinfeld, J. H. *Science* **1997**, *276*, 96.

(4) Buth, R.; Hoyermann, K.; Seeba, J. *25th Symp. Combust.* **1994**, 841.

(5) Berho, F.; Lesclaux, R. *Chem. Phys. Lett.* **1997**, *279*, 289.

(6) Berho, F.; Caralp, F.; Rayez, M.-T.; Lesclaux, R.; Ratajczak, E. *J. Phys. Chem. A* **1998**, *102*, 1.

(7) Hansen, K. B.; Wilbrandt, R.; Pagsberg, P. *Rev. Sci. Instrum.* **1979**, *50*, 1532.

(8) Wallington, T. J.; Japar, S. M. *J. Atmos. Chem.* **1989**, *9*, 399.

(9) Wallington, T. J.; Dagaut, P. D.; Kurylo, M. J. *Chem. Rev.* **1992**, *92*, 667.

(10) (a) Baerends, E. J.; Ellis, D. E.; Ros, P. *Chem. Phys.* **1973**, *2*, 41. (b) Te Velde, G.; Baerends, E. J. *J. Comput. Phys.* **1992**, *99*, 84.

(11) Vosko, S. H.; Wilk, L.; Nusair, M. *Can. J. Phys.* **1980**, *58*, 1200.

(12) Perdew, J. P.; Chevary, J. A.; Vosko, S. H.; Jackson, K. A.; Pederson, M. R.; Singh, D. J.; Fiolhais, C. *Phys. Rev. B* **1992**, *46*, 6671.

(13) Baulch, D. L.; Duxbury, J.; Grant, S. J.; Montague, D. C. *J. Phys. Chem. Ref. Data* **1981**, *10*, Suppl. 1.

(14) Kajii, Y.; Obi, K.; Nakashima, N.; Yoshihara, K. *J. Chem. Phys.* **1987**, *87*, 5059.

(15) Schuler, R. H.; Buzzard, G. K. *Int. J. Radiat. Phys. Chem.* **1997**, *8*, 563.

(16) Sehested, K.; et al. Private communication, 1998.

(17) Wallington, T. J.; Hurley, M. D. *Chem. Phys. Lett.* **1992**, *189*, 437.

(18) DeMore, W. B.; Sander, S. P.; Golden, D. M.; Hampson, R. F.; Kurylo, M. J.; Howard, C. J.; Ravishankara, A. R.; Kolb, C. E.; Molina, M. J. Jet Propulsion Laboratory Publication 97-4, Pasadena, CA, 1997.

(19) Kaiser, E. W.; Wallington, T. J. *J. Phys. Chem.* **1996**, *100*, 9788.

(20) Langer, S.; Ljungström, E.; Wängberg, I.; Wallington, T. J.; Hurley, M. D.; Nielsen, O. J. *Int J. Chem. Kinet.* **1996**, *28*, 299.

(21) Wine, P. H.; Semmes, D. H. *J. Phys. Chem.* **1983**, *87*, 3572.

(22) Kishino, T.; Kobayashi, K. *Water Res.* **1996**, *30* (2), 387.

(23) Takasuka, M.; Matsui, Y. *J. Chem. Soc., Perkin Trans. 2* **1979**, 1743.

(24) Braun, W.; Herron, J. T.; Kahaner, D. K. *Int. J. Chem. Kinet.* **1988**, *20*, 51.

(25) McMillan, D. F.; Golden, D. M. *Annu. Rev. Phys. Chem.* **1982**, *33*, 493.

(26) Atkinson, R.; Baulch, D. L.; Cox, R. A.; Hampson, R. F., Jr.; Kerr, J. A.; Troe, J. *J. Phys. Chem. Ref. Data* **1992**, *21*, 1125.

(27) NIST/EPA Gas Phase Infrared Database, Version 1.0, Gaithersburg, MD, 1992.

(28) Silverstein, R. M.; Bassler, G. C.; Morrill, T. C. *Spectrometric Identification of Organic Compounds*, 5th ed.; John Wiley and Sons: New York, 1991.

(29) Carter, W. P. L. *J. Air Waste Manag. Assoc.*, **1994**, *44*, 881.